Dependence of surface stress, surface energy and surface tension on potential and charge

— Supplementary information —

Electronic Supplementary Information (ESI) of Phys. Chem. Chem. Phys.

DOI of the main article: **10.1039/b710065e**

Dominik Kramer[*]
Institut für Nanotechnologie (INT), Forschungszentrum Karlsruhe,
Postfach 3640, 76021 Karlsruhe, Germany

Table S1: Examples of either linear $f(q)$ or parabolic $f(E)$ surface stress response to charging

Figures S1, S2 and S3.

[*] Corresponding author. Tel.: +49 +7247 82 6379, Fax.: +49 +7247 82 6368
E-mail address: Dominik.Kramer@int.fzk.de (D. Kramer)

Table S1. Examples of either linear $f(q)$ or parabolic $f(E)$ surface stress response to charging. Other published surface stress curves are more complex, *e.g.* showing slope changes or several extrema like those in [3,38,65]. Unless noted otherwise, measurements have been done with polycrystalline electrodes.

Electrode		Electrolyte	Appearance	Ref.	1st Autor	Year
Au	ribbon	0.1 M KCl	parabolic	Fig. 2 of [4]	Beck	1969
Au Pt	1 µm film on glass 1 µm film on glass	0.1 M KCl, $1.67 \cdot 10^{-3}$ N H_2SO_4	partially parabolic	Fig. 1 of [13], Fig. 2 of [13]	Fredlein	1971
Pb	1.2 mm piece	0.15 M KBr + 0.5 M Na_2SO_4	partially parabolic (linear df/dq)	Fig. 1.3 of [58] (Fig. 4 of [59])	Gokhshtein	1971
Au	1 µm film on glass	$HClO_4$	parabolic	Fig. 5 of [12]	Fredlein	1974
Au	ribbon	K_2SO_4	parabolic	Figs. 4 and 12 of [14]	Lin	1976
Pt	25 µm strip	0.05 M H_2SO_4	parabolic	Fig. 3 of [15]	Pangarov	1978
Au	90 µm foil on piezo	0.8 M NaF	roughly parabolic	Fig. 2 of [66]	Fredlein	1979
C	porous	5 M NaCl	parabolic	Figs. 2, 4, 5 of [16]	Oren	1986
C	12 cm porous piece	5 M NaCl	parabolic	Fig. 4 of [17]	Golub	1987
Au	film on quartz	2 mM KF	parabolic	Fig. 5 of [64]	Jaeckel	1994
Au	film on quartz	0.1 M K_2SO_4	parabolic	Figs. 6 and 8 of [19]	Láng	1995
Au Pt	50 nm film 60 nm film	0.1 M KCl 0.1 M $NaClO_4$ + NaOH	parabolic parabolic	Fig. 2 (a) of [18] Fig. 2 (b) of [18]	Raiteri	1995
Au	100 nm film on quartz	$KClO_4$ + x mM pyridine	partially parabolic	Figs. 3, 5, 6, 7 of [63]	Efimov	1996
Au(111)	200 nm film on glass	0.1 M H_2SO_4 +1 mM $CuSO_4$ + 1 mM (CsBr or CsCl)	linear $f(q)$ ($I(E) \propto f(E)$)	Figs. 2 and 3 of [40]	Haiss	1996
Au(111)	30 nm film on cantilever	0.1 M KCl	parabolic	Fig. 2 of [22] and Fig. 2 of [23]	O'Shea, Brunt	1996
Metal	jellium model	1-1 electrolyte	parabolic	Fig. 1 of [20]	Schmickler	1998
Au	0.25 mm plate	$HClO_4$, $KClO_4$	partially parabolic (linear df/dq)	Figs. 4 and 5 of [42]	Valincius	1998
Au(111)	single crystal	0.1 M $HClO_4$	linear $f(q)$	Fig. 3 of [31]	Ibach	1999
Au(100)	single crystal	0.1 M $HClO_4$	parabolic	Fig. 4 of [31]	Ibach	1999
Au(111)	200 nm film on glass	0.1 M $HClO_4$, 1 M H_2SO_4, 0.1 M $HClO_4$ + 5 mM CsCl	linear $f(q)$	Fig. 2 of [28], Fig. 5 of [29], Fig. 18 of [30]	Haiss	1998, 2002, 2001
Pt	porous, nanocrystalline	1 M KOH, 0.5 M H_2SO_4	linear $f(q)$	Fig. 2. of [2], Fig. 3. of [2]	Weissmüller	2003
Au	porous	0.05 M H_2SO_4.	linear $f(q)$	Fig. 2 of [32]	Kramer	2004
Pt	porous, nanocrystalline	0.02 M…1 M NaF	linear $f(q)$	Fig. 2 of [33]	Viswanath	2005
Pt	150 nm film on glass	1 M $HClO_4$ 0.8 M HCOOH 1 M H_2SO_4 0.8 M HCOOH	parabolic parabolic	Fig. 3 c of [24] Fig. 7 b of [24]	Láng	2005
Au(111)	100 nm film on silicon	0.1 M $HClO_4$	linear $f(q)$	Fig. 29 of [34]	Tabard-Cossa	2005
Pt	porous, nanocrystalline	0.7 M NaF	linear $f(q)$	Figs. 5 and 8 of [35]	Viswanath	2007

Fig. S1. Schematic illustration of two states of an electrode, described by the independent parameters γ and A, and of two paths of parameter variation.

γ is a function of the potential, it decreases if an uncharged electrode is charged. Due to the conservation of energy, different reversible ways to change the state of the electrode from its initial values γ_0 and A_0 to γ and A_1 will require the same total energy.

A) For the path A, the surface of area A_0 is charged starting at the *pzc* (blue dot), followed by a change in area at constant potential (and at constant γ), *e.g.* by reversible cleavage of a crystal. During this step, the electrical work $q\phi\,(A_1 - A_0)$ is done by the potentiostat which keeps the potential at the given value ϕ, in addition to the mechanical work $\gamma\,(A_1 - A_0)$ required to do the change in area. For the path B, the surface area is increased first, at the constant potential $\phi = 0$. For A, the work done is $W_{\mathrm{A}} = A_0\omega + (A_1 - A_0)\gamma + q\phi(A_1 - A_0)$, for path B, $W_{\mathrm{B}} = (A_1 - A_0)\gamma_0 + A_1\omega$, with $\omega = \omega(\phi)$ being the electrical work per area of charging of the surface starting from $q = 0$, Eq. (15) and Eq. (16).

B) The diagram is simpler if unit areas are considered. In that case, the surface energy of the unit area (red dot at $A_1 = 1$) is seen to be given by Eq. (18).

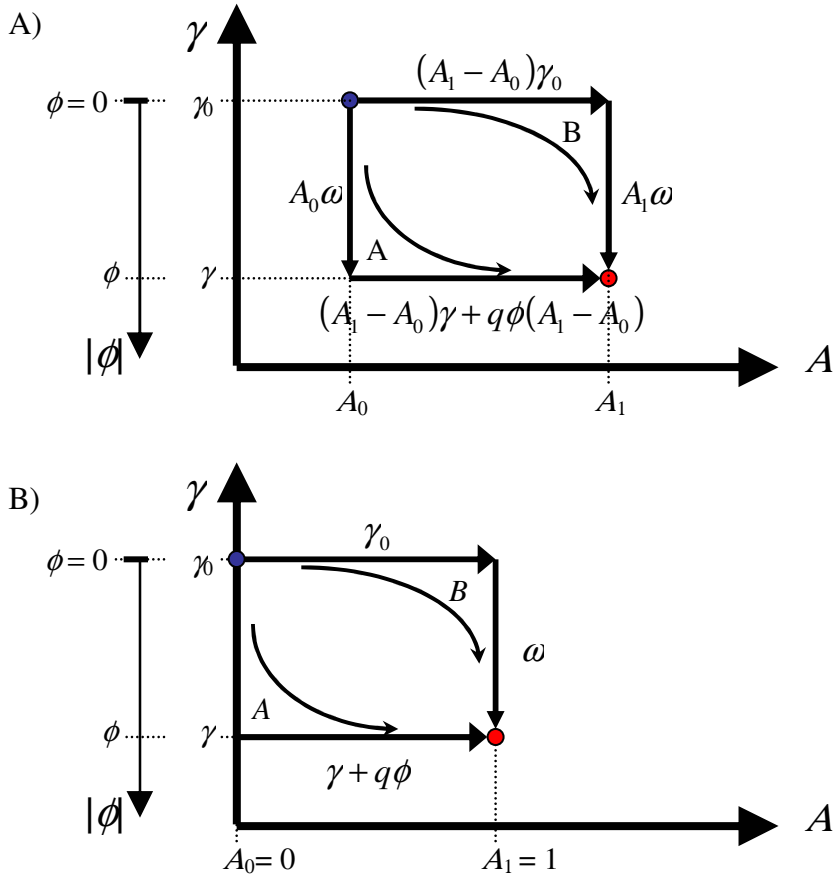

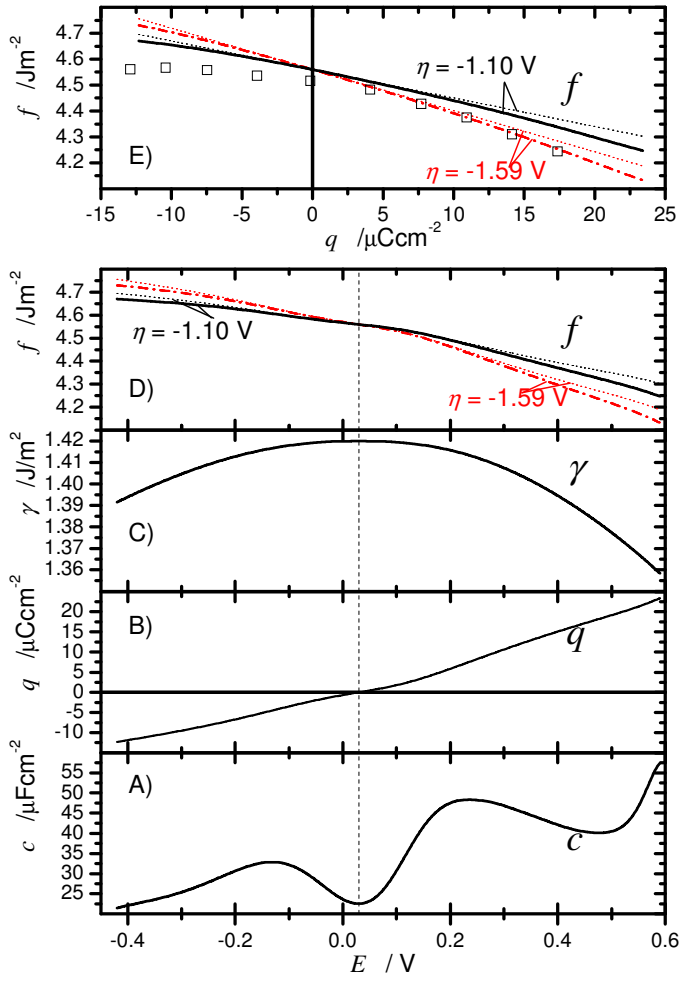

Fig. S2: Application of the model to the unreconstructed Au(100) surface, demonstrating the effect of different values of η.

A) Double layer capacity curve of an Au(100) surface in 10 mM $HClO_4$, after lifting of the reconstruction by a potential sweep. Data values taken from Fig. 3(a) of [56].

B) Charge density q obtained by integration of A).

C) Surface tension $\gamma(E)$ obtained by integration of B) and by using the vacuum value of the surface tension at the *pzc*, γ_0 = 1.42 J/m^2 [30], neglecting that γ_0 of the solid-liquid phase will differ from the vacuum value.

D) and **E)** Surface stress f of the Au(100) surface according to the model, Eq. (46), calculated using $k = 0.1$ for weak adsorption. Perchlorate is considered weakly adsorbing, but specific adsorption occurs on gold [56], therefore, this low but nonzero k value seems reasonable. Black curves: $\eta = -1.10$ V. Red cuves: $\eta = -1.59$ V, which is the $\Delta f/\Delta q$ value given by IBACH, based on a fit of experimental data with straight line for positive charge only [31]. At the *pzc*, the vacuum surface stress value, f_0 = 4.56 J/m^2,[30] has been used. The squares in E) are have been obtained by adding a constant to the experimental Δf values given by IBACH [31]. The dotted lines give the ηq part of f, demonstrating that the surface tension term of Eq. (46) is much smaller than ηq. Since the surface stress of the uncharged surface is large, the maximum relative variation $\Delta f / f$ is still less than 10%.

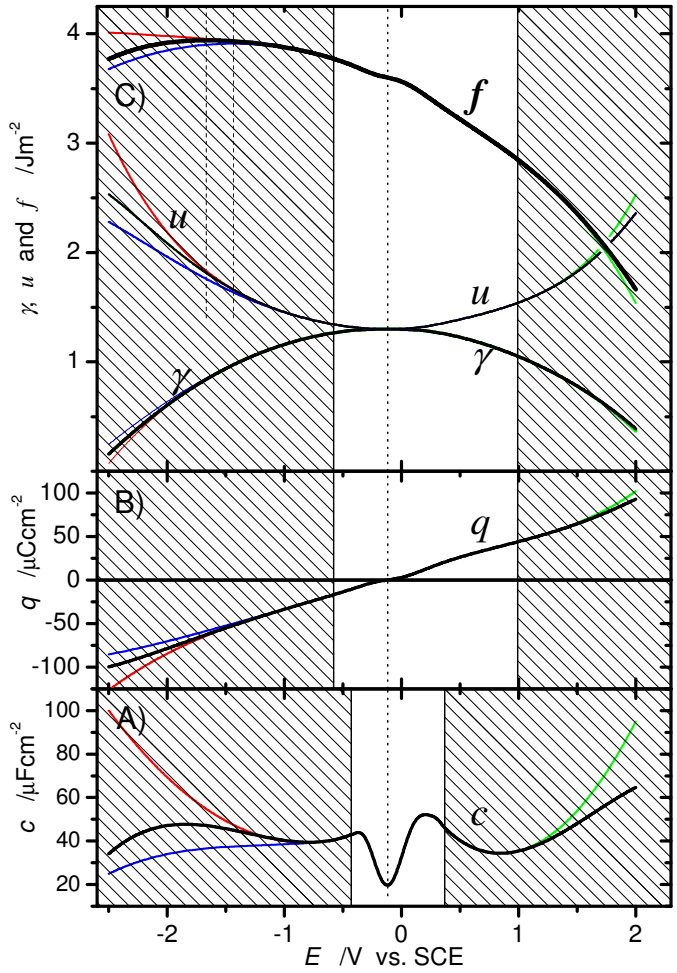

Fig. S3: Demonstration of some important consequences of the model

i) The predicted $f(E)$ is roughly parabolic, which is apparent here due to the huge potential window of the graph. The approximation of f to a ideal parabola is not as good as that of γ which is almost parabolic. *ii*) The maximum of f can be shifted considerably compared to the maximum of γ at the *pzc* (by more than 1.3 V and by more than 2.5 Jm^{-2} for the example shown here). *iii*) Within the accessible potential window, the variation of f can be much larger than that of γ.

The shaded areas of B) and C) are intended to indicate potentials which are hardly accessible in aqueous solutions.

A) Capacitance of the double layer which is used to predict γ and f. The values of the non-shaded area have been taken from the Fig. 3(c) of [56] and correspond to the capacity of an (unreconstructed) Au(210) surface in 10 mM $HClO_4$. The curves within the shaded area of A) are different arbitrary extrapolations.

B) Charge densities q obtained by integration of the capacitances of A).

C) Surface tension γ obtained by integration of the charge densities B) and by assuming $\gamma_0 = 1.3\ Jm^{-2}$, surface energy u according to Eq. (18) (neglecting adsorption) and surface stress f according Eq. (46) of the simple toy model and by assuming $f_0 = 3.6\ Jm^{-2}$, $k = 0.1$ (weak adsorption) and $\eta = -1.2$ V.